

Scaling LLaNA: Advancing NeRF-Language Understanding Through Large-Scale Training

Andrea Amaduzzi, Pierluigi Zama Ramirez, Giuseppe Lisanti, Samuele Salti, Luigi Di Stefano

CVLAB, University of Bologna

<https://andreamaduzzi.github.io/llana/>

Abstract—Recent advances in Multimodal Large Language Models (MLLMs) have shown remarkable capabilities in understanding both images and 3D data, yet these modalities face inherent limitations in comprehensively representing object geometry and appearance. Neural Radiance Fields (NeRFs) have emerged as a promising alternative, encoding both geometric and photorealistic properties within the weights of a simple Multi-Layer Perceptron (MLP). This work investigates the feasibility and effectiveness of ingesting NeRFs into an MLLM. We introduce LLaNA, the first MLLM able to perform new tasks such as NeRF captioning and Q&A, by directly processing the weights of a NeRF’s MLP. Notably, LLaNA is able to extract information about the represented objects without the need to render images or materialize 3D data structures. In addition, we build the first large-scale NeRF-language dataset, composed by more than 300K NeRFs trained on ShapeNet and Objaverse, with paired textual annotations that enable various NeRF-language tasks. Based on this dataset, we develop a benchmark to evaluate the NeRF understanding capability of our method. Results show that directly processing NeRF weights leads to better performance on NeRF-Language tasks compared to approaches that rely on either 2D or 3D representations derived from NeRFs.

Index Terms—Neural Fields, NeRF, LLM, NeRF Captioning, NeRF QA, NeRF Zero-shot Classification

I. INTRODUCTION

The field of Natural Language Processing has been profoundly transformed by Large Language Models (LLMs) [1]–[4], due to their text comprehension and generation capabilities. These results have fostered the development of Multimodal LLMs (MLLMs) [5]–[9], which can process various modalities such as images, videos and audio, to generate text describing and reasoning about the content of such modalities. Recently, MLLMs have also been extended to 3D data [10]–[12], primarily represented as colored point clouds, yielding remarkable results even in this scenario.

Another approach for representing objects and scenes has emerged alongside traditional images and 3D data: Neural Radiance Fields (NeRFs) [13]. NeRFs are coordinate-based neural networks, typically Multi-Layer Perceptrons (MLPs), designed to capture both the geometry and the photorealistic appearance of an object. By learning a continuous radiance field across 3D space, NeRFs can be used to generate realistic images from any viewpoint or reconstruct the object’s 3D surface by querying the trained model. Using NeRFs to represent 3D data offers distinct advantages over conventional approaches like multi-view images or point clouds. The continuous nature of NeRFs allows generating unlimited photorealistic images at any desired resolution while only requiring

the storage of MLP weights rather than a large collection of images. Due to their benefits, NeRFs are effectively becoming a new modality stored and communicated independently, with datasets of NeRFs being made publicly available [14], [15] and companies providing digital twins of objects represented as NeRFs.

The increasing adoption of NeRFs and their appealing characteristics prompted us to investigate the following research question: is it possible to build an MLLM able to directly ingest NeRFs? Inspired by recent studies on meta-networks that can process neural fields [15], [16], we answer this question positively by showing that it is possible to process the weights of a given NeRF with a meta-network encoder that projects the NeRF weights into the embedding space of a pre-trained LLM such as LLaMA 2 [4]. By doing so, we create the first MLLM for NeRFs, dubbed Large Language and NeRF Assistant (LLaNA), which can perform NeRF-language tasks such as NeRF captioning, NeRF Q&A and zero-shot NeRF classification.

In the former version of this paper [17], we introduced ShapeNeRF-Text, the first NeRF-language dataset, comprising language annotations for 40K objects from ShapeNet. To collect this dataset, we designed an automated annotation framework that leverages MLLMs to produce text annotations for NeRFs trained on 3D models. Using this dataset alongside an additional split containing manually curated textual descriptions [18], we established a benchmark for NeRF textual assistants. Building upon such a foundation, this work introduces several key advances: first, we significantly expand the scale and diversity of NeRF-language understanding by introducing ObjaNeRF-Text, a new dataset of NeRFs, built upon Objaverse [19]. With 280K annotated NeRFs, this new dataset represents a seven-fold increase in scale compared to ShapeNeRF-Text. While ShapeNeRF-Text was limited to synthetic objects from 10 classes of ShapeNet with machine-generated annotations, ObjaNeRF-Text provides two key improvements: it enlarges the variety of synthetic objects and introduces real-world objects, while also incorporating high-quality human-written annotations from [10] and [11], providing a higher quality and more diverse benchmark for NeRF-language understanding. Secondly, we extend our previous experimental setup by investigating the LLM scaling effects on NeRF-language tasks. These experiments provide valuable insights into how the size of the underlying LLM influences the performance of MLLMs in processing and understanding 3D neural fields. When evaluating LLaNA, we compare it against

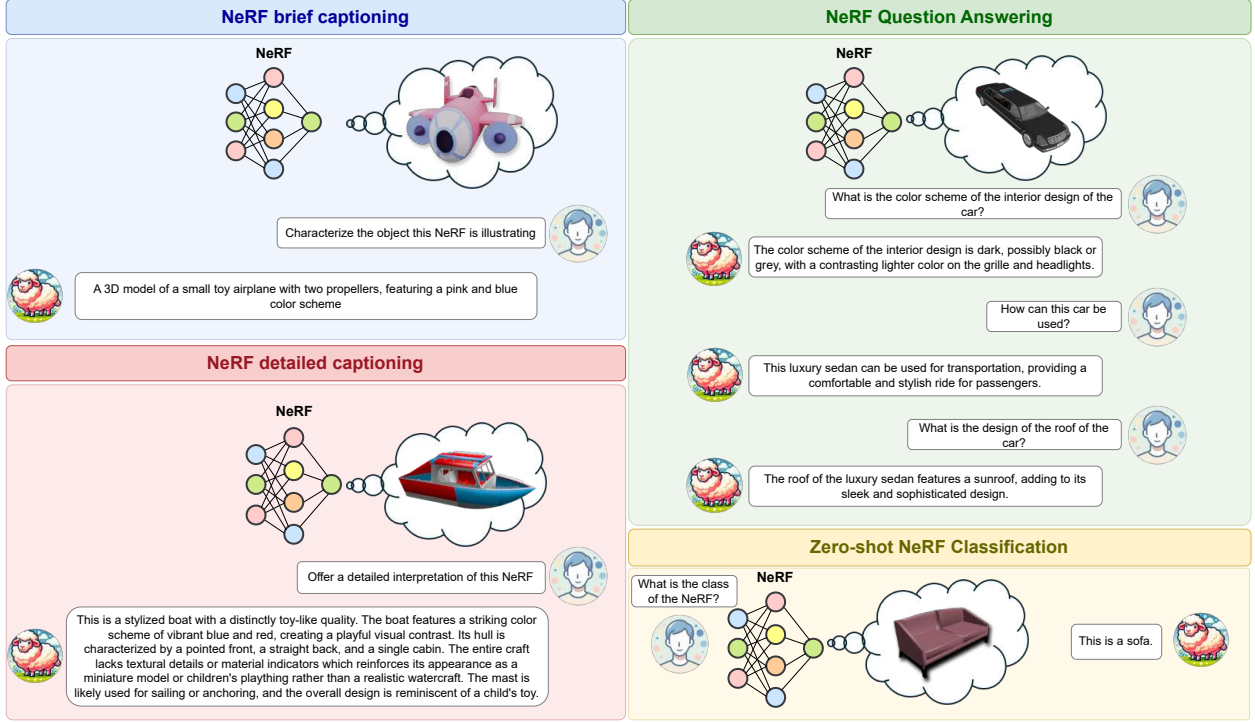


Fig. 1: **LLaNA**. A new Multimodal Large Language Model that understands and reasons on an input NeRF. Notably, our framework processes directly the NeRF weights and performs tasks such as captioning, Q&A, and zero-shot classification of NeRFs.

traditional approaches that process NeRFs by first converting them to explicit data representations – either rendered images or 3D point clouds – and then using existing MLLMs designed for these modalities. Through a comprehensive evaluation on our proposed benchmark, we demonstrate the advantages of our direct NeRF processing approach. We show that the quality of MLLM outputs is adversely affected by both the resolution of extracted 3D geometry and images, as well as the choice of the viewpoint used for image rendering. Important details might be lost by rendering from the wrong angle, or the extracted geometry might not be detailed enough. Vice versa, by operating directly on the MLP weights, we are able to extract all the information about the object without any other design decision. Our approach turns out to be the most effective way to create a NeRF assistant, as it consistently outperforms MLLMs processing images or 3D geometries extracted by querying NeRFs.

The key differences with [17] are:

- We create **ObjaNeRF-Text**, the largest existing NeRF-Language dataset, providing 280K NeRFs paired with textual annotations sourced from [10] and [11], with a seven-fold increase in scale over **ShapeNeRF-Text** [17]. This new dataset expands the variety of synthetic objects and incorporates real-world objects. Moreover, unlike the machine-generated textual annotations of **ShapeNeRF-Text**, the test set of **ObjaNeRF-Text** features high-quality human-written conversations, providing more natural and reliable ground-truth data.

- We explore the impact of the LLM size on NeRF understanding by extending our previously proposed model **LLaNA** to utilize **LLAMA-13b**, offering new insights into how LLM size affects performance on NeRF-language tasks.

The summary of our contributions is:

- **LLaNA**, the first MLLM capable of performing tasks such as captioning and Q&A on NeRFs.
- We show that it is possible to build such an assistant by directly processing the NeRFs weights with a meta-encoder, which is faster and captures more information compared to rendering images or extracting 3D data.
- A **NeRF-Language** benchmark for MLLMs, built on **ShapeNet** and **Objaverse**, which contains more than 320K NeRFs of synthetic and real objects, paired with text annotations. Our evaluation on this benchmark demonstrates that **LLaNA** outperforms traditional MLLMs operating on discrete representations derived from NeRFs.
- An analysis of the impact of the LLM size on MLLMs evaluated on NeRF-Language tasks.

II. RELATED WORK

Multimodal Large Language Models. Significant advancements have been made by Large Language Models (LLMs) in language understanding, reasoning, and generalization capabilities [1]–[4]. These models have been extended into Multimodal Large Language Models (MLLMs), which broaden their reasoning abilities by including other modalities

like images [5], [6], [20], [21], audio [22], and videos [9], [23]. MLLMs generally align target features with the corresponding textual ones and then incorporate them into LLMs to perform various text-based inference tasks. Some MLLMs are trained entirely from scratch [24], [25], others utilize pretrained LLMs [7], [8], [26]–[28]. 3D MLLMs focus on understanding the 3D world typically represented in one of two ways: as colored point clouds [10]–[12], [29], [30] or multi-view images [31]. These models use different training approaches - some learn from 2D images [12], [29], [31], while others are trained by directly matching text descriptions with points [10], [11], [30].

Neural radiance fields. NeRF [13] have been applied in several visual tasks such as novel view synthesis [32], generative media [33], and robotics [34]. The base formulation employs MLPs to convert spatial coordinates into colors and densities. Recent advancements substitute or enhance MLPs with explicit data structures [35]–[38] for faster training and inference.

Neural radiance fields and language. The interaction between NeRF and language has been recently investigated for several practical applications. Many works address the problem of generating geometrically consistent views of objects or scenes described by textual prompts [33], [39]–[44]. Other approaches focus on editing the scene represented by a NeRF through text, e.g., by changing the appearance and shape of objects [45]–[52], or by inserting/removing objects in the scene [53], [54]. Some techniques investigate new types of radiance fields that predict language features for each spatial location alongside density and color [55], [56]. By transferring knowledge from vision-language models into these enhanced radiance fields, they can be queried by textual prompts. Such *language fields* are parametrized by a neural network. Unlike all previous methods, the solution proposed in [57] is the first to utilize the weights of a NeRF’s MLP as an input modality. This method aims to learn a mapping between the embedding spaces of the NeRF and CLIP [58] to perform tasks such as NeRF retrieval from textual or image queries. Differently, our goal is to develop an MLLM capable of reasoning about NeRFs.

Deep learning on neural networks. Several studies have explored using meta-networks, i.e., neural networks that process other neural networks. Initially, researchers concentrated on predicting network characteristics, such as accuracy and hyperparameters, by processing their weights [59]–[63]. Several recent works focus on processing networks that implicitly encode data, e.g., Implicit Neural Representations (INR) or Neural Fields. These methods are able to classify or segment data by processing solely the weights of the input neural networks. Functia [64] trains a single shared network on a full dataset to learn compact modulation embeddings for each sample, which can then be used for various downstream tasks. More recent research has shifted focus to analyzing networks that represent individual data samples, such as networks trained to model specific objects. By leveraging a novel encoder architecture for MLP weights, `inr2vec` [65] extracts compact embeddings from INRs of 3D shapes, which are employed as inputs for downstream tasks. `nf2vec` [15] extends

`inr2vec` to ingest the NeRF’s network weights to classify, segment, or retrieve similar NeRFs. The solution from [66] develop a strategy to process neural fields represented by a hybrid tri-plane structure. Other approaches [67]–[70] develop equivariant architectures to handle MLPs by exploiting weight space symmetries [71] as an inductive bias. Also, Graph Neural Networks have been investigated to compute a network representation [16], [72]. Since we aim to process NeRFs directly from the network weights, we employ `nf2vec` as our meta-encoder due to its efficient and scalable architecture.

III. METHODOLOGY

This section describes the proposed Large Language and NeRF Assistant (LLaNA). We first provide an overview of NeRFs and the meta-encoder that maps NeRF weights into a global embedding. Then, we present the overall LLaNA framework and discuss our training protocol.

Neural Radiance Fields A Neural Radiance Field (NeRF) [13] is a framework that employs coordinate-based neural networks, typically Multi-Layer Perceptrons (MLP), to model 3D scenes or objects. It is trained on a set of images taken from various vantage points. Once trained, the NeRF can be exploited to perform novel views synthesis, i.e., photorealistic rendering of images from viewpoints unseen at training time.

In its base formulation, the MLP is a function of continuous 3D coordinates $\mathbf{p} = (x, y, z) \in \mathbb{R}^3$, that yields four-dimensional outputs, $RGB\sigma \in [0, 1]^4$. This output encodes the RGB color and the volume density σ at each 3D location in the scene. The volume density σ can be interpreted as the differential probability of a ray terminating at a point \mathbf{p} . After training, a NeRF can render images from any desired viewpoints at arbitrary resolution by querying it for the values of RGB and σ at several points along the ray corresponding to each pixel and applying the volumetric rendering equation [13].

In this work, we implement NeRFs as MLPs composed of L hidden layers, an input layer, and an output layer. An example of MLP with 1 input, 1 output, and 1 hidden layer is shown in Fig. 2 (left). A layer is parameterized by a weight matrix plus a bias vector. More in detail, the hidden layers in our architecture have the same number of input and output neurons, H , thus having squared weight matrices $\mathbf{W}_l \in \mathbb{R}^{H \times H}$ for $l = 1, \dots, L$ and H -dimensional biases $\mathbf{b}_l \in \mathbb{R}^H$. The input \mathbf{p} goes through a 24-frequency encoding [13], therefore the first layer has $\mathbf{W}_{in} \in \mathbb{R}^{144 \times H}$ and $\mathbf{b}_{in} \in \mathbb{R}^H$. The final layer has $\mathbf{W}_{out} \in \mathbb{R}^{H \times 4}$ and $\mathbf{b}_{out} \in \mathbb{R}^4$. Adopting the same architecture used in [15], an instance of the employed NeRF has $L = 3$ hidden layers, with 64 neurons each. The *ReLU* activation function is applied between all layers except for the last one, which directly computes the density and RGB values without any activation function. Our NeRFs are trained using a Smooth L_1 loss [73] between the predicted and ground-truth RGB pixel intensities, weighting background pixels less than foreground pixels (0.8 foreground vs. 0.2 background). The final rendered images are obtained by querying the neural network with 3D coordinates to obtain

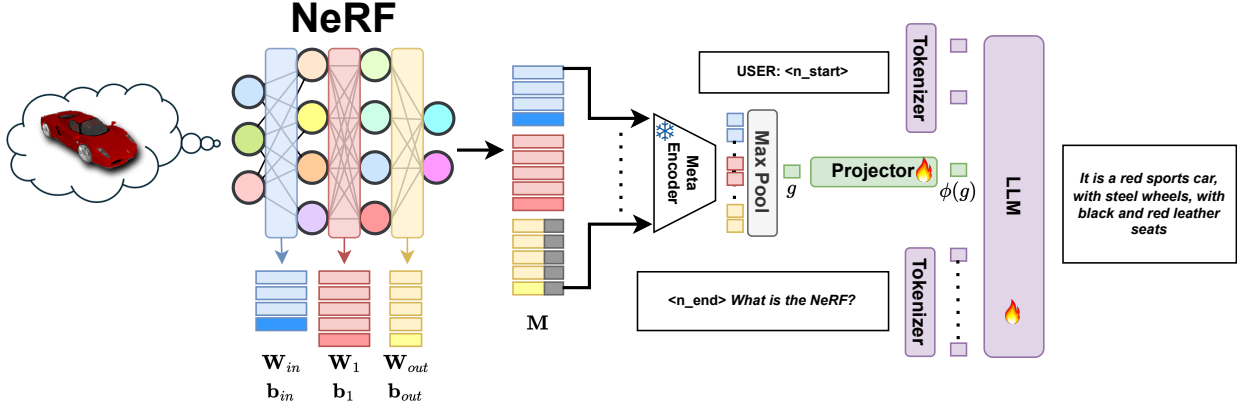


Fig. 2: Framework overview. Example of NeRF captioning.

RGB color values and density estimates. These values are then integrated along camera rays using volumetric rendering techniques [13], to produce the final image. Each NeRF is trained for approximately 2000 steps, until it achieves good reconstruction quality as measured by the Peak Signal-to-Noise Ratio (PSNR).

Meta-encoder In this work, we investigate how to design a Multimodal Large Language Model (MLLM) that works directly on the weights of NeRFs. We expect the NeRF weights to contain comprehensive information about the represented object, such as its geometry and appearance. Thus, an encoder could extract all the relevant information from these weights to perform language-based tasks like generating captions and answering questions about the object.

Inspired by the recent development of meta-networks capable of processing neural fields [15], [16], we employ *nf2vec* [15] as our meta-encoder architecture. This approach takes as input the weights of a NeRF and provides as output a global embedding that distills the content of the input. In particular, the weight matrices and biases of the input NeRF are stacked along the row dimension to form a matrix $\mathbf{M} \in \mathbb{R}^{S \times H}$, where $S = 144 + 1 + L * (H + 1) + H + 1 = L * H + L + H + 146$. Before stacking, we pad the weights and biases of the output layer, \mathbf{W}_{out} and \mathbf{b}_{out} , with zeros to obtain H columns (see Fig. 2, center).

The meta-encoder is parametrized as an MLP with batch normalization layers [74] and *ReLU* non-linearities. To gracefully scale with the MLP input dimensions, the encoder processes each row of \mathbf{M} independently, extracting a total of S tokens, each of length G , from an input NeRF. Then, they are processed by a max-pooling layer to provide a global representation $g \in \mathbb{R}^G$ of the NeRF, with $G = 1024$ in our experiments. The encoder has been pre-trained on the NeRFs from ShapeNeRF-Text and ObjaNeRF-Text by applying the self-training protocol of *nf2vec* [15], i.e., jointly with a decoder architecture that, given as input the NeRF global embedding, reconstructs the same images as the input NeRF from arbitrary viewpoints.

Large Language and NeRF Assistant Inspired by recent approaches that proposed effective Multimodal Large Language Models, we build LLaNA by leveraging on a pre-trained

LLM with a Transformer backbone [75], in our experiments LLaMA 2 [4], and projecting the NeRF modality into its embedding input space, as proposed for images and 3D data [7], [10] (see Fig. 2, right). Thanks to the self-attention mechanism, the transformer can understand the contextual relationships between the text and the NeRF tokens, enabling it to generate responses based on both the text and the NeRF inputs.

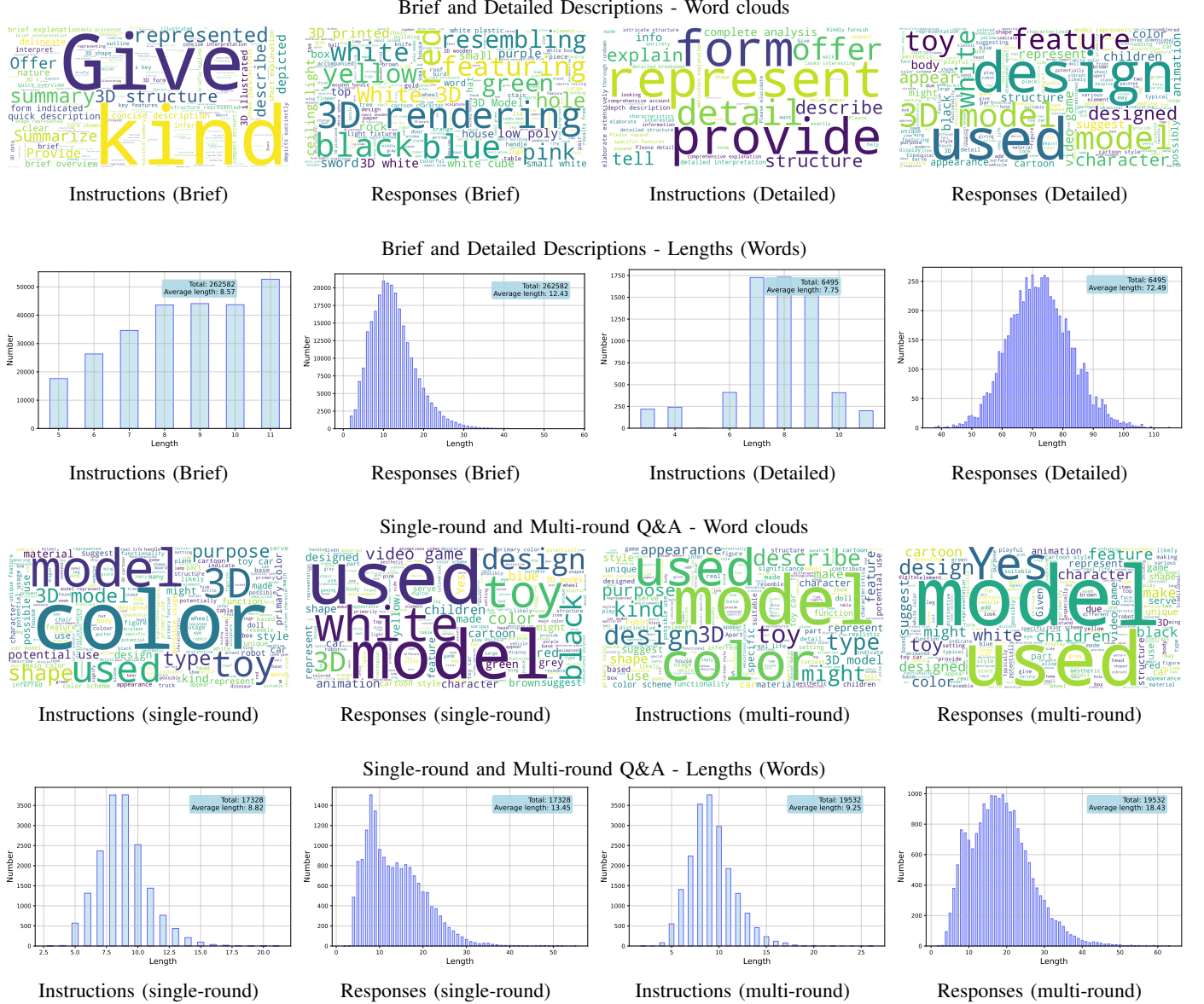
We define a projector network, ϕ , composed of a stack of 3 trainable linear layers, interleaved with *GeLU* activation functions, that project the embedding of the input NeRF computed by the meta-encoder into the embedding space of LLaMA 2. More in detail, the NeRF embedding is encapsulated between two special tokens, $\langle n_start \rangle$ and $\langle n_end \rangle$, whose embeddings are learned end-to-end while training.

Finally, an input sequence composed by the NeRF embedding and k word tokens, $(\langle n_start \rangle, \phi(g), \langle n_end \rangle, w_1, w_2, \dots, w_k)$, is provided as input to the LLM which predicts a sequence of word tokens $(\hat{w}_{k+1}, \hat{w}_{k+2}, \dots, \hat{w}_{eos})$.

Training protocol To train our framework, we hold multiple conversations about each NeRF leveraging both our ShapeNeRF-Text and ObjaNeRF-Text datasets (see Section IV). These conversations are organized into a set of prompts from the user and expected ground-truth answers that are used to optimize the original auto-regressive objective of the LLM. For the meta-encoder, we train *nf2vec* on the NeRFs of ShapeNeRF-Text and ObjaNeRF-Text for 100 epochs on 4 NVIDIA A100 GPUs. When training LLaNA we follow a two-stage training protocol, keeping the *nf2vec* weights frozen:

Stage1: projector training. In the first stage, we train the projector network ϕ to align the NeRF and the word embedding spaces while keeping the LLM weights fixed. We train on an instruction dataset of brief descriptions from ShapeNeRF-Text and ObjaNeRF-Text to learn the projection layer efficiently. We also train the embeddings of the special tokens used to encapsulate the NeRF one. We optimize the projector weights and the embeddings for 3 epochs with a learning rate of 0.002 and a batch size of 16 on each GPU.

Stage2: instruction tuning. The second stage of training

Fig. 3: **ObjaNeRF-Text** statistics of ground-truth text annotations

focuses on teaching the model to understand and reason about NeRF data using three types of text from ShapeNeRF-Text and ObjaNeRF-Text: brief descriptions, detailed descriptions, and Q&A conversations. In this phase, we optimize both the projector and the LLM for 3 epochs. We employ a learning rate of 0.00002 and a batch size of 4 on each GPU.

Our model is implemented in PyTorch and trained on NVIDIA A100 GPUs with 64GB of VRAM each. The model variant based on the 7B LLAMA architecture requires 4 GPUs for training, while our largest version, which uses the 13B LLAMA architecture, needs 8 GPUs. Training either version of the model takes approximately one day to complete.

IV. BENCHMARK

To train and validate our NeRF assistant, we created a dataset of NeRFs with textual annotations. It features objects from ShapeNet [76] and Objaverse [19].

A. *ObjaNeRF-Text* dataset

ObjaNeRF-Text is built leveraging on the rendered views from G-Buffer Objaverse [77]. This dataset provides high-quality rendered views of a subset of 280K models from Objaverse. Each object was captured from 40 different camera positions: 38 views taken around the object at two different elevation angles, plus one view from above and one from below. We train a NeRF on each object, leveraging these rendered views and following the procedure detailed in Section III

B. *ShapeNeRF-Text* dataset

The textual annotations of ObjaNeRF-Text are derived from the dataset proposed in [10]. This work provides machine-generated textual annotations for Objaverse models, divided into three categories: brief descriptions, detailed descriptions and Q&A conversations. The brief descriptions are concise captions of the object, taking into account its global structure

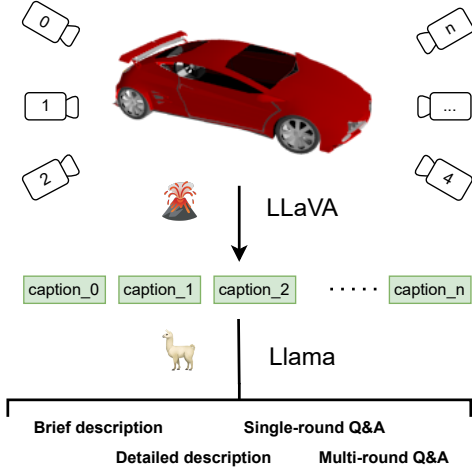


Fig. 4: **Automatic annotation pipeline.** Given a 3D model, N views are rendered and processed by a VLM (LLaVA) to generate view-specific captions. These are aggregated by an LLM (LLaMA) for final descriptions and Q&A.

and appearance. Detailed descriptions are longer sentences that describe all the details of the object. The single-round Q&As consist of a question about the object and the corresponding ground-truth answer, while the multi-round Q&As are longer conversations formed by 3 questions and the relative answers. Objaverse provides colored meshes of both synthetic and real-world scanned objects. When building ObjNeRF-Text, we identified the intersection between the 280K objects in G-Buffer Objaverse and the 3D models from this textually annotated dataset. Overall, the training set of ObjNeRF-Text comprises around 280K 3D models with brief descriptions, and 30K complex text annotations including detailed descriptions and Q&A conversations, associated with 7K different objects. For our evaluation benchmark, we created two different test sets: one for comparison with PointLLM [10] and another for comparison with GPT4Point [11], leveraging the splits proposed in these works. This dualsplit approach was necessary to ensure the largest and most fair evaluation possible since many samples in the test set of PointLLM were used to train GPT4Point. The final test sets contain human-annotated captions for 1366 objects in the PointLLM test set and 518 objects in the GPT4Point test set. To facilitate the training and test of LLaNA, the words of the original text annotations referring to the point cloud data structure, such as “point cloud”, “3D point cloud” or “cloud of points” have been modified into “NeRF”.

Statistical details of ObjNeRF-Text As for the training set, the average lengths in words for the instructions/responses are 8.57/12.43 for brief descriptions, 7.75/72.49 for detailed descriptions, 8.82/13.45 for single-round Q&As and 9.25/18.43 for multi-round Q&As. Fig. 3 shows histograms of the instruction/response length and the word clouds obtained after removing generic words such as “model”, “object” and “NeRF”, emphasizing frequent words in the ground-truth instructions and responses.

As quantitatively assessed in Section V-C, many of the

questions belonging to the Q&A set require a holistic 3D understanding of the object, to be answered correctly.

ShapeNeRF-Text is the NeRF-Language dataset proposed in [17]. This dataset provides 40K NeRFs of objects from ShapeNet, paired with language annotations. These ground-truth conversations have been automatically generated by leveraging LLaVA [7] and LLAMA [4]. More in detail, a *brief description*, a *detailed description*, 3 *single-round Q&As*, and one *multi-round Q&A* have been generated for every object. Our automatic data annotation pipeline is inspired by Cap3D [78]. First, multiple views of each ShapeNet object have been rendered from different perspectives. Then, each view has been provided as input to LLaVA (LLaVA2-13b) [7] to get a detailed description of the object from that point of view. Subsequently, starting from the captions generated by LLaVA, LLaMA 3 (LLaMA3-8B-chat) was used to generate the final ground-truth text data. An overview of this process is provided in Fig. 4.

C. Language tasks and metrics

The experimental results on ShapeNeRF-Text and ObjNeRF-Text are reported divided by tasks: brief captioning, detailed captioning and single-round Q&A. Since the test sets of ObjNeRF-Text contain short human-annotated captions, such results fall into the brief captioning category. Furthermore, for this task, we also evaluate the methods on the GPT2Shape Human Shape Text (HST) dataset [18], a subset of ShapeNet for which human-curated brief descriptions are publicly available. We employ standard language similarity metrics to evaluate these methods. We compute the cosine similarity between the global embeddings of the generated and ground-truth sentences provided by the pre-trained encoders Sentence-BERT [79] and SimCSE [80]. These metrics based on learned networks are the most effective in measuring the quality of the generated output [10]. We also include standard handcrafted metrics based on n-gram statistics, like BLEU-1 [81], ROUGE-L [82], and METEOR [83].

V. EXPERIMENTAL RESULTS

As our method is the first to investigate language tasks on NeRF, there are no baselines in the literature. However, given a NeRF, a straightforward way to create an assistant for it could be to render an image and use a MLLM capable of ingesting images. Alternatively, we could extract the 3D shape from the NeRF and use one of the recent 3D MLLMs. Hence, we evaluate LLaVA (v1.6) [7] and BLIP-2 [84] for images, as well as PointLLM [10] and GPT4Point [11] for colored point clouds. Since NeRFs can render arbitrary viewpoints after training, we also include the evaluation of LLaVA [7] in a multi-view scenario. More in detail, we render images from N viewpoints randomly sampled between the set of camera poses used to train each NeRF; then, we concatenate tokens from these N images and fed them into LLaVA alongside text instructions. We set $N=3$ because the model cannot process a higher number of images correctly. In addition, we test 3D-LLM [12], which processes meshes and multi-view images. When evaluating the baselines on ShapeNeRF-Text

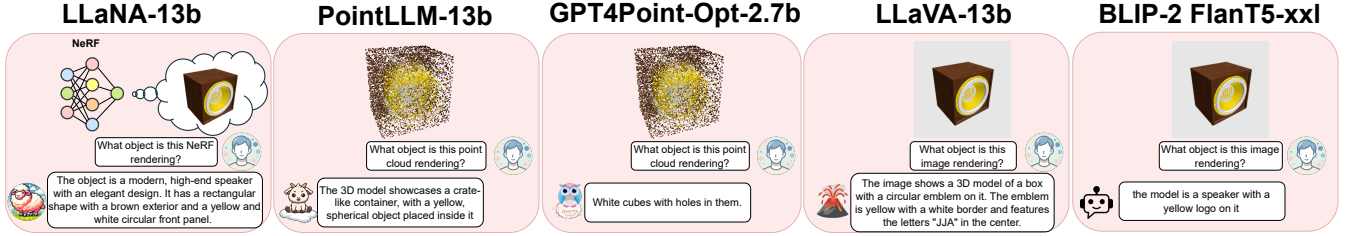


Fig. 5: Qualitative results on ShapeNeRF-Text brief descriptions.

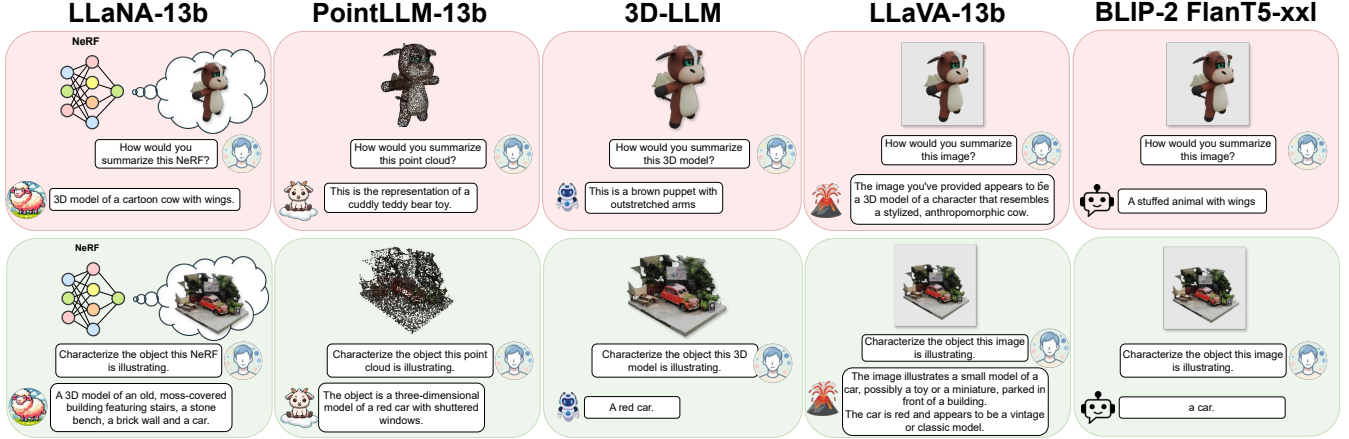


Fig. 6: Qualitative results on ObjNeRF-Text brief descriptions (PointLLM test set).

and ObjNeRF-Text, we employ the official code and pre-trained models released by the respective authors¹.

A. Experiments on ObjNeRF-Text and ShapeNeRF-Text

Tables I, II, V, VI and VII show the results on ShapeNeRF-Text, while Tables III and IV show the results on ObjNeRF-Text. The textual annotations of the ObjNeRF-Text test sets consist of short descriptions, making them suitable for the evaluation of the brief captioning task. In all tables, the baselines are ordered by increasing the size of the underlying LLM.

a) *Brief captioning*: We report the results for the brief description task on ShapeNeRF-Text, HST and ObjNeRF-Text in Table I, Table II, Table III and Table IV. When evaluating image-based methods on ObjNeRF-Text, we used random object views since Objaverse 3D models lack consistent orientation, making it impossible to identify standard front and back views as in ShapeNeRF-Text.

LLaNA-13b consistently outperforms all other models across all metrics, often by large margins against runners-up. Moreover, in most cases, the second best performing model is LLaNA-7b, thus the same architecture with a smaller LLM. The difference in the quality of the caption generated by LLaNA compared to the baselines is showcased by the

TABLE I: NeRF brief captioning on ShapeNeRF-Text. Best results are in **bold**, runner-up is underlined. (FV: front-view, BV: back-view, MV: multi-view)

| Model | Modality | S-BERT | SimCSE | BLEU-1 | ROUGE-L | METEOR |
|--------------------|-------------|--------------|--------------|--------------|--------------|--------------|
| GPT4Point-Opt-2.7b | Point cloud | 41.85 | 40.22 | 11.76 | 16.54 | 11.63 |
| 3D-LLM FlanT5-xl | Mesh + MV | 59.46 | 56.42 | 12.69 | 21.49 | 14.32 |
| LLaVA-vicuna-7b | Image (FV) | <u>59.85</u> | <u>62.35</u> | 22.67 | <u>23.24</u> | <u>23.35</u> |
| LLaVA-vicuna-7b | Image (BV) | 55.68 | 58.46 | 21.97 | 22.46 | 22.50 |
| LLaVA-vicuna-7b | Image (MV) | 59.77 | 61.42 | <u>23.16</u> | 22.68 | 23.01 |
| PointLLM-7b | Point cloud | 49.59 | 48.84 | 16.74 | 17.92 | 14.56 |
| LLaNA-7b | NeRF | 74.94 | 76.41 | 42.73 | 43.64 | 41.95 |
| BLIP-2 FlanT5-xxl | Image (FV) | 56.13 | 58.21 | 5.46 | 18.69 | 9.67 |
| BLIP-2 FlanT5-xxl | Image (BV) | 52.48 | 54.05 | 5.67 | 18.20 | 9.50 |
| LLaVA-vicuna-13b | Image (FV) | <u>61.00</u> | <u>61.16</u> | 14.30 | 20.00 | <u>23.31</u> |
| LLaVA-vicuna-13b | Image (BV) | 54.35 | 56.09 | 21.94 | 21.67 | 22.09 |
| LLaVA-vicuna-13b | Image (MV) | 59.64 | 61.01 | <u>22.84</u> | <u>22.17</u> | 23.08 |
| PointLLM-13b | Point cloud | 51.54 | 50.35 | 17.20 | 18.51 | 14.92 |
| LLaNA-13b | NeRF | 75.09 | 76.45 | 42.83 | 43.70 | 42.21 |

qualitative results reported in Figures 5, 6, and 7 where the descriptions provided by LLaNA are the most accurate.

A clear trend in the tables and qualitative results is that image-based models tend to perform better than models processing point clouds. This is likely due to the larger amount of data used during training of the modality encoder, i.e. millions of images versus hundreds of thousands of shapes, which enhances their generalization ability, as well as the capability of images to capture more details than point clouds at the input resolutions required by image-based MLLMs versus 3D MLLMs. Nonetheless, our method, which operates on NeRFs, benefits from a holistic view of the object and provides the most accurate descriptions. Remarkably, in LLaNA, all the necessary information for this language task can be extracted from a single global embedding obtained

¹LLaVA: <https://github.com/haotian-liu/LLaVA> BLIP-2: <https://github.com/salesforce/LAVIS/tree/main/projects/blip2>
PointLLM: <https://github.com/OpenRobotLab/PointLLM>
GPT4Point: <https://github.com/Pointcept/GPT4Point>
3D-LLM: <https://github.com/UMass-Foundation-Model/3D-LLM>

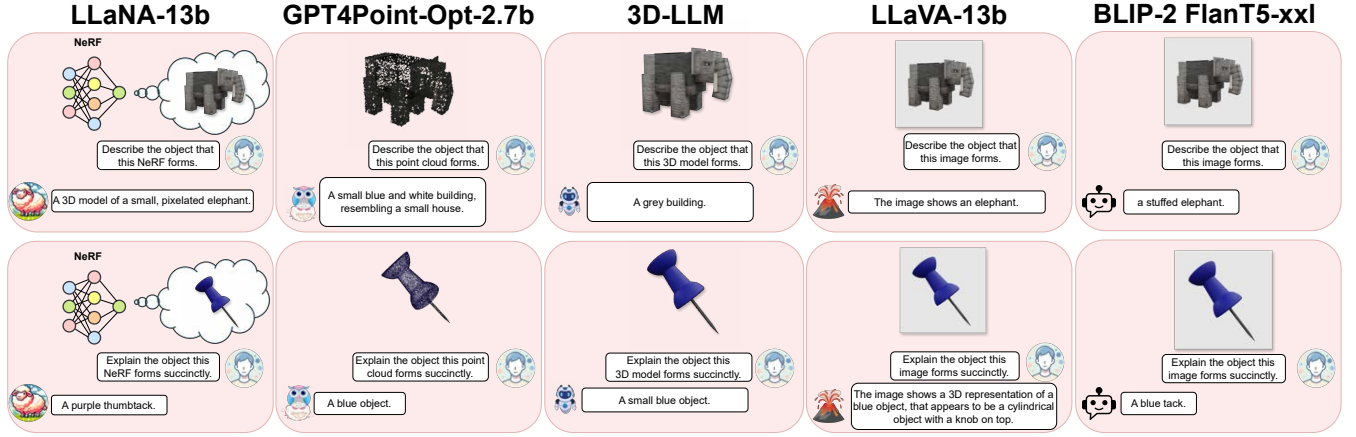


Fig. 7: Qualitative results on ObjNeRF-Text brief descriptions (GPT4Point test set).

TABLE II: NeRF brief captioning on the HST dataset.

Best results are in **bold**, runner-up is underlined.

(FV: front-view, BV: back-view, MV: multi-view)

| Model | Modality | S-BERT | SimCSE | BLEU-1 | ROUGE-L | METEOR |
|--------------------|-------------|--------------|--------------|--------------|--------------|--------------|
| GPT4Point-Opt-2.7B | Point cloud | 43.15 | 42.22 | 12.02 | 18.73 | 13.69 |
| 3D-LLM FlanT5-xl | Mesh + MV | <u>56.07</u> | 52.13 | <u>15.94</u> | <u>20.71</u> | <u>15.22</u> |
| LLaVA-vicuna-7b | Image (FV) | 54.31 | 56.28 | 10.08 | 14.71 | 14.53 |
| LLaVA-vicuna-7b | Image (BV) | 51.75 | 52.29 | 8.13 | 13.96 | 14.18 |
| LLaVA-vicuna-7b | Image (MV) | 54.15 | <u>56.87</u> | 10.32 | 12.76 | 15.13 |
| PointLLM-7b | Point cloud | 43.40 | 44.50 | 8.53 | 11.64 | 9.97 |
| LLaNA-7b | NeRF | 64.78 | 65.01 | 20.65 | 23.24 | 24.10 |
| BLIP-2 FlanT5-xxl | Image (FV) | <u>57.11</u> | <u>59.43</u> | 8.21 | <u>18.02</u> | 12.14 |
| BLIP-2 FlanT5-xxl | Image (BV) | 54.11 | 56.37 | 9.09 | 17.38 | 11.79 |
| LLaVA-vicuna-13b | Image (FV) | 55.62 | 55.56 | 6.56 | 11.81 | 14.52 |
| LLaVA-vicuna-13b | Image (BV) | 50.00 | 50.79 | 9.39 | 12.76 | 14.46 |
| LLaVA-vicuna-13b | Image (MV) | 54.25 | 55.56 | <u>9.78</u> | 14.13 | 14.99 |
| PointLLM-13b | Point cloud | 45.41 | 46.39 | 9.57 | 12.38 | 11.92 |
| LLaNA-13b | NeRF | 65.66 | 66.09 | 20.80 | 24.28 | 25.90 |

TABLE III: NeRF brief captioning on ObjNeRF-Text (PointLLM test set).

Best results are in **bold**, runner-up is underlined.

(RV: random view, MV: multi-view)

| Model | Modality | S-BERT | SimCSE | BLEU-1 | ROUGE-L | METEOR |
|-------------------|-------------|--------------|--------------|--------------|--------------|--------------|
| 3D-LLM FlanT5-xl | Mesh + MV | 38.22 | 39.60 | 5.47 | 7.29 | 10.75 |
| LLaVA-vicuna-7b | Image (RV) | 39.29 | 40.93 | 5.22 | 8.35 | 12.49 |
| LLaVA-vicuna-7b | Image (MV) | <u>40.15</u> | <u>41.09</u> | <u>5.62</u> | <u>9.07</u> | <u>13.22</u> |
| PointLLM-7b | Point cloud | 38.81 | 40.11 | 5.55 | 8.39 | 11.24 |
| LLaNA-7b | NeRF | 41.36 | 42.28 | 13.21 | 16.93 | 15.63 |
| BLIP-2 FlanT5-xxl | Image (RV) | 35.48 | 35.19 | <u>7.69</u> | <u>13.75</u> | 11.68 |
| LLaVA-vicuna-13b | Image (RV) | 38.57 | 39.05 | 4.62 | 7.63 | 11.85 |
| LLaVA-vicuna-13b | Image (MV) | <u>41.01</u> | <u>41.10</u> | 4.87 | 8.03 | <u>12.35</u> |
| PointLLM-13b | Point cloud | 39.64 | 40.63 | 5.94 | 8.43 | 11.63 |
| LLaNA-13b | NeRF | 42.08 | 42.40 | 13.86 | 17.51 | 16.18 |

by directly processing the NeRF weights. Comparing the results of image-based MLLMs when processing front versus back views, we can see that the vantage point has a non-negligible effect on the performance of such baselines, with SentenceBERT and SimCSE metrics diminishing by about 4 points in all baselines. In a dataset without canonical poses for objects, this would be a relevant limitation that processing NeRF weights seamlessly sidesteps. Finally, we observe that the multi-view setup of LLaVA provides better performance to the single-view counterpart. Regarding LLM size scaling, our analysis reveals only marginal performance improvements with larger models in brief captioning tasks. On ShapeNeRF-Text, LLaVA shows a minimal improvement in S-BERT scores

TABLE IV: NeRF brief captioning on ObjNeRF-Text (GPT4Point test set).

Best results are in **bold**, runner-up is underlined.

(RV: random view, MV: multi-view)

| Model | Modality | S-BERT | SimCSE | BLEU-1 | ROUGE-L | METEOR |
|--------------------|-------------|--------------|--------------|--------------|--------------|--------------|
| GPT4Point-Opt-2.7b | Point cloud | 34.42 | 31.89 | 8.76 | <u>13.62</u> | 13.55 |
| 3D-LLM FlanT5-xl | Mesh + MV | 41.26 | 37.74 | <u>11.08</u> | 12.26 | 15.58 |
| LLaVA-vicuna-7b | Image (RV) | 41.59 | 42.38 | 7.24 | 11.74 | 16.01 |
| LLaVA-vicuna-7b | Image (RV) | <u>42.34</u> | <u>43.21</u> | 8.59 | 11.94 | <u>18.52</u> |
| LLaNA-7b | NeRF | 43.73 | 43.09 | 20.22 | 25.15 | 22.21 |
| BLIP-2 FlanT5-xxl | Image (RV) | 37.24 | 37.32 | <u>10.63</u> | <u>16.87</u> | 14.69 |
| LLaVA-vicuna-13b | Image (RV) | 42.08 | 41.04 | 6.53 | 10.57 | 15.67 |
| LLaVA-vicuna-13b | Image (MV) | <u>44.15</u> | <u>43.19</u> | 6.75 | 10.86 | <u>16.10</u> |
| LLaNA-13b | NeRF | 44.26 | 43.75 | 20.61 | 25.62 | 22.36 |

from 59.85 to 61.00 when using the 13B parameter model, while other metrics actually deteriorate. Similarly, PointLLM exhibits modest gains of approximately 1 point across metrics, and LLaNA demonstrates even smaller improvements. This trend is consistent across HST and ObjNeRF-Text datasets. These findings suggest that the ability to perform NeRF-language tasks is not strongly correlated with LLM size. Unlike traditional NLP tasks, where larger models generally lead to significant performance boosts due to their enhanced language understanding and generation capabilities, NeRF-based captioning appears to depend more on the model’s ability to process and integrate 3D and visual information from the input NeRF. Given the substantial computational costs of training and deploying larger models, the minimal performance gains observed in brief captioning tasks may not justify the increased resource demands. Another key observation is that the quality of the input encoding and the processing pipeline, which turns NeRF representations into LLM-compatible features, have a greater impact on performance than increasing the size of the underlying LLM. For example, despite using LLMs of similar sizes (2.7B for GPT4Point and 3B for 3D-LLM), these models exhibit very different performance levels. One possible explanation is that these tasks require precise spatial and geometric reasoning, which may not inherently improve with a larger LLM. Models like 3D-LLM, which incorporate multi-view processing and colored meshes, likely benefit more from their specialized architecture than from parameter scaling.

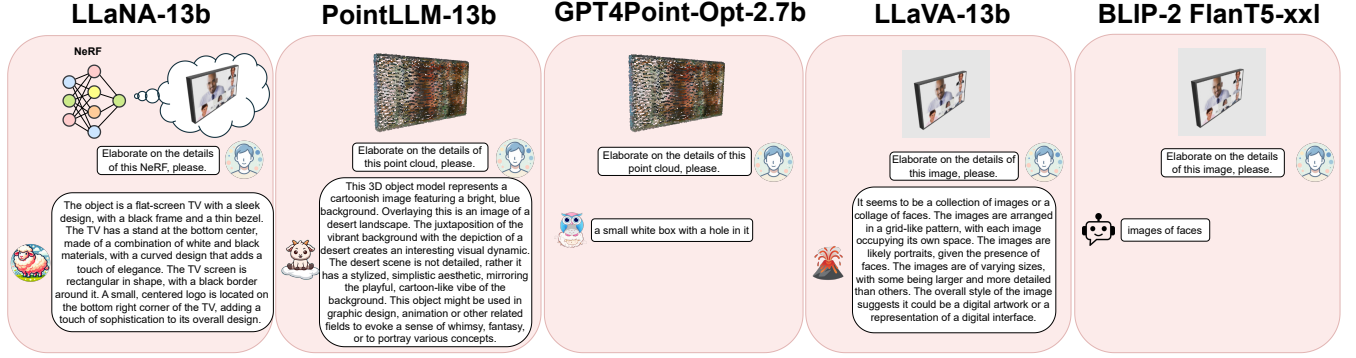


Fig. 8: Qualitative results on ShapeNeRF-Text detailed descriptions. From top to bottom: brief and detailed descriptions, single-round Q&A

TABLE V: NeRF detailed captioning on ShapeNeRF-Text. Best results are in **bold**, runner-up is underlined. (FV: front-view, BV: back-view, MV: multi-view)

| Model | Modality | S-BERT | SimCSE | BLEU-1 | ROUGE-L | METEOR |
|--------------------|-------------|--------------|--------------|--------------|--------------|--------------|
| GPT4Point-Opt-2.7b | Point cloud | 42.44 | 38.33 | 3.72 | 9.21 | 5.13 |
| 3D-LLM FlanT5-xl | Mesh + MV | 58.00 | 53.91 | 1.58 | 14.40 | 5.28 |
| LLaVA-vicuna-7b | Image (FV) | 57.55 | 57.68 | 14.99 | 22.82 | 14.36 |
| LLaVA-vicuna-7b | Image (BV) | 53.11 | 54.46 | 14.73 | 22.47 | 14.05 |
| LLaVA-vicuna-7b | Image (MV) | 55.26 | 58.46 | 15.07 | 24.05 | 14.85 |
| PointLLM-7b | Point cloud | 59.02 | 58.30 | 10.28 | 19.26 | 10.55 |
| LLaNA-7b | NeRF | 75.25 | 77.42 | 19.57 | 32.96 | 20.45 |
| BLIP-2 FlanT5-xxl | Image (FV) | 41.27 | 40.69 | 0.18 | 7.83 | 2.60 |
| BLIP-2 FlanT5-xxl | Image (BV) | 38.49 | 37.89 | 0.19 | 7.72 | 2.58 |
| LLaVA-vicuna-13b | Image (FV) | 59.08 | 58.87 | 23.63 | 23.55 | 22.55 |
| LLaVA-vicuna-13b | Image (BV) | 50.09 | 50.33 | 13.77 | 21.36 | 13.18 |
| LLaVA-vicuna-13b | Image (MV) | <u>60.21</u> | 59.51 | 15.07 | 32.16 | 14.64 |
| PointLLM-13b | Point cloud | 59.64 | 58.55 | 10.52 | 19.44 | 10.83 |
| LLaNA-13b | NeRF | 75.51 | 77.63 | <u>19.87</u> | 32.93 | <u>20.46</u> |

TABLE VI: NeRF single-round Q&A on ShapeNeRF-Text. Best results are in **bold**, runner-up is underlined. (FV: front-view, BV: back-view, MV: multi-view)

| Model | Modality | S-BERT | SimCSE | BLEU-1 | ROUGE-L | METEOR |
|--------------------|-------------|--------------|--------------|--------------|--------------|--------------|
| GPT4Point-Opt-2.7b | Point cloud | 27.62 | 31.41 | 6.26 | 9.38 | 5.41 |
| 3D-LLM FlanT5-xl | Mesh + MV | 69.62 | 67.55 | 32.19 | 40.95 | 35.83 |
| LLaVA-vicuna-7b | Image (FV) | 71.79 | 71.96 | 25.79 | 34.04 | 34.86 |
| LLaVA-vicuna-7b | Image (BV) | 70.88 | 70.93 | 25.17 | 33.30 | 34.22 |
| LLaVA-vicuna-7b | Image (MV) | 72.26 | 70.67 | 24.09 | 34.67 | 35.64 |
| PointLLM-7b | Point cloud | <u>74.70</u> | <u>74.40</u> | <u>36.81</u> | <u>44.41</u> | <u>39.76</u> |
| LLaNA-7b | NeRF | 81.03 | 81.61 | 45.98 | 53.27 | 49.97 |
| BLIP-2 FlanT5-xxl | Image (FV) | 45.20 | 47.92 | 11.50 | 20.16 | 13.49 |
| BLIP-2 FlanT5-xxl | Image (BV) | 45.06 | 47.66 | 11.50 | 19.98 | 13.44 |
| LLaVA-vicuna-13b | Image (FV) | 71.61 | 70.98 | 20.19 | 30.42 | 32.53 |
| LLaVA-vicuna-13b | Image (BV) | 68.25 | 69.06 | 20.03 | 29.84 | 32.27 |
| LLaVA-vicuna-13b | Image (MV) | 71.84 | 71.16 | 20.04 | 30.20 | 33.46 |
| PointLLM-13b | Point cloud | <u>74.65</u> | <u>74.18</u> | <u>37.16</u> | <u>44.86</u> | <u>40.13</u> |
| LLaNA-13b | NeRF | 81.05 | 81.60 | 46.08 | 53.44 | 49.98 |

b) *Detailed captioning*: The results for the detailed captioning task are presented in Table V. LLaNA demonstrates superior performance compared to all other models, showing significant improvements in data-driven metrics such as Sentence-BERT and SimCSE. For traditional metrics like BLEU-1, ROUGE-L, and METEOR, our model achieves comparable results to LLaVA. 3D-LLM [12], processing multi-view images and colored meshes, performs well on the Sentence-BERT metric, whereas all other metrics show poor results. Interestingly, the point-based model PointLLM [10] performs similarly to the image based one, LLaVA [7]. Considering the Sentence-BERT metric, LLaNA-13b achieves 75.51, notably 15.87 points more than PointLLM and 15.30 points more than LLaVA-13b multi-view setup. These substantial performance gaps suggest that, while individual or aggregated images may be sufficient for brief descriptions, they may lack all the details needed to provide a comprehensive description. Moreover, the dependency of the output quality on the selected vantage points remains strong, as proven by the varying performance achieved by LLaVA across front-view, back-view, and multi-view scenarios. In contrast, the NeRF weights contain detailed and complete information about the object, which is fundamental for more granular description tasks, with the additional advantage of not requiring tuning such hyperparameters. The ability of NeRF to capture holistic information about the object is also shown in Fig. 8, where only the direct processing of NeRF weights lets LLaNA understand that the

object is a TV. PointLLM and LLaVA provide detailed but wrong descriptions, likely because of the need to extract the intermediate discrete representation as a point cloud or an image, losing information. Indeed, in both cases, it is hard even for a human observer to provide the right description from the intermediate modalities shown in the figure. When comparing the different versions of our model, the 13B variant slightly outperforms its 7B counterpart, a pattern consistently observed across other models in the table, such as PointLLM and LLaVA. Specifically, the relative improvements from 7B to 13B versions on Sentence-BERT and SimCSE are: 0.62 and 0.25 for PointLLM, 1.53 and 1.19 for LLaVA, 0.26 and 0.21 for LLaNA. This limited performance gain suggests that the architectural improvements and training strategies employed in these models may be more crucial for performance than simply scaling up model size, as also observed with the results obtained in the brief captioning task. Regarding the training strategies of these models, an interesting observation can be made. Overall, the highest performance on NeRF detailed captioning is achieved by LLaNA, LLaVA, and PointLLM; notably, the only models incorporating LLM fine-tuning in their training protocol. This pattern strongly suggests that fine-tuning the LLM plays a crucial role in enhancing the quality of the generated descriptions. While this fine-tuning stage appears less critical for generating brief captions, it significantly impacts the quality of longer, detailed descriptions. This can be attributed to the ability of the fine-tuned LLM to

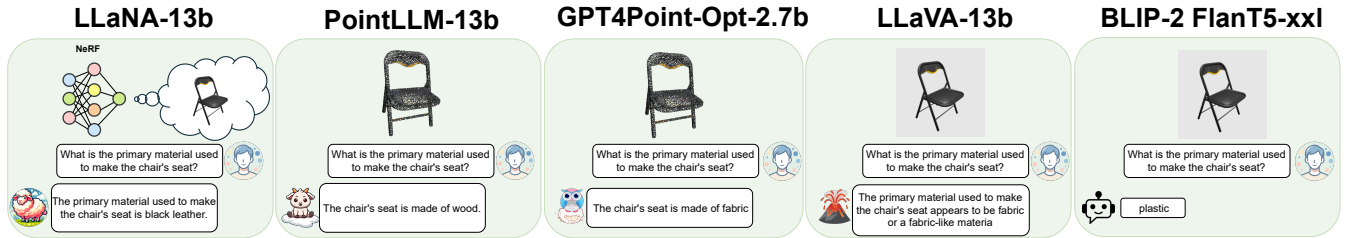


Fig. 9: Qualitative results on ShapeNeRF-Text single-round Q&A.

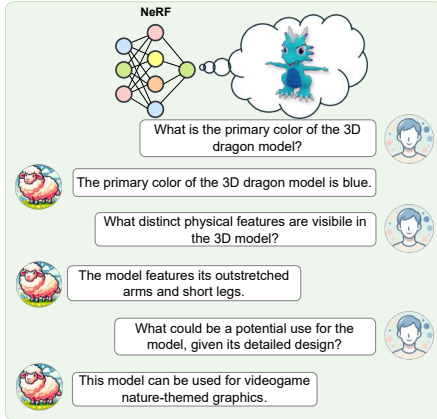


Fig. 10: NeRF multi-round Q&A example from ObjaNeRF-Text.

adapt its pre-trained language understanding capabilities to the specific characteristics and vocabulary of NeRF-based object descriptions.

c) *single-round Q&A*: In the single-round Q&A experiment, we test the ability of the assistants to provide accurate answers to specific questions about the object. We prompt the models with the NeRF, or the image/cloud extracted from it, followed by one of the questions in the single-round Q&A annotations associated with the NeRF. We then collect the answer generated by the model and compare it against the ground-truth answer with the selected metrics. Results are reported in Table VI. Interestingly, PointLLM [10] performs better than LLaVA [7] in this task, likely because it has been specifically trained to answer detailed questions about objects represented as point clouds. Nevertheless, LLaNA maintains its position as the top-performing method across all metrics by substantial margins, mirroring our findings from the brief and detailed captioning tasks. Using the 13B LLAMA backbone, the performance gaps between LLaNA and the second-best model, PointLLM, are large: 6.40 for Sentence-BERT, 7.42 for SimCSE, 8.92 for BLEU-1, 8.58 for ROUGE-L, and 9.85 for METEOR. Notably, these margins remain consistently large even when using the 7B LLAMA backbone. The performance advantage of LLaNA shows that our meta-encoder and projector architecture are capable of effectively extracting fine-grained information from the NeRF representation, even if they are processing directly NeRF

TABLE VII: Zero-Shot NeRF Classification.

Best results are in **bold**, runner-up is underlined. (FV: front-view, BV: back-view, MV: multi-view)

| Model | Modality | Accuracy (%) |
|--------------------|-------------|--------------|
| GPT4Point-Opt-2.7b | Point cloud | 41.93 |
| 3D-LLM FlanT5-xl | Mesh + MV | 60.55 |
| LLaVA-vicuna-7b | Image (FV) | 60.25 |
| LLaVA-vicuna-7b | Image (BV) | 57.00 |
| LLaVA-vicuna-7b | Image (MV) | 67.25 |
| PointLLM-7b | Point cloud | 50.14 |
| LLaNA-7b | NeRF | 67.56 |
| BLIP-2 FlanT5-xxl | Image (FV) | 63.67 |
| BLIP-2 FlanT5-xxl | Image (BV) | 61.47 |
| LLaVA-vicuna-13b | Image (FV) | 66.13 |
| LLaVA-vicuna-13b | Image (BV) | 63.90 |
| LLaVA-vicuna-13b | Image (MV) | 73.45 |
| PointLLM-13b | Point cloud | 48.72 |
| LLaNA-13b | NeRF | <u>69.27</u> |

weights. Remarkably, the amount of information they can extract lets LLaNA answer more precisely than when images or point clouds are extracted from the NeRF. Indeed, as shown in Fig. 9 which reports a qualitative example from ShapeNeRF-Text, the only assistant able to answer correctly to a precise question about the material of the chair is LLaNA. Finally, another qualitative result confirming the ability of LLaNA to provide high-quality answers to specific questions, in this case in a multi-round Q&A experiment where a human user asks questions on a NeRF from the test set of ObjaNeRF-Text, is reported in Fig. 10. Similar to our findings with brief and detailed descriptions, the Q&A results show minimal performance difference between LLaNA-13B and LLaNA-7B, further reinforcing that MLLM performance on these tasks is not strongly dependent on the size of the underlying language model. Furthermore, the consistently superior performance of LLaNA, LLaVA, and PointLLM across both tasks underscores the critical role of LLM finetuning in developing models that can effectively describe and answer questions regarding 3D objects.

d) *Zero-shot classification*: We compare assistants on the task of zero-shot classification. We query the models with the sentence “What is the class of the NeRF/image/cloud? Choose among these: [ShapeNet classes]” where [ShapeNet classes] are the 10 ShapeNet classes available in ShapeNeRF-Text. We consider the answer correct only if the ground truth class appears in the response. We report results in Table VII on ShapeNeRF-Text. Using multiple views boosts

TABLE VIII: **NeRF brief captioning on ShapeNeRF-Text**. All methods trained on ShapeNeRF-Text training set. Best results are in **bold**, runner-up is underlined. (FV: front-view, MV: multi-view)

| Model | Modality | S-BERT | SimCSE | BLEU-1 | ROUGE-L | METEOR |
|--------------------|-------------|--------------|--------------|--------------|--------------|--------------|
| GPT4Point-Opt-2.7b | Point cloud | 37.96 | 39.00 | 21.33 | 22.29 | <u>24.88</u> |
| PointLLM-7b | Point cloud | <u>55.48</u> | <u>57.28</u> | <u>21.67</u> | <u>25.84</u> | <u>24.54</u> |
| LLaNA-7b | NeRF | 76.04 | 77.13 | 45.00 | 45.87 | 44.52 |
| LLaVA-vicuna-13b | Image (FV) | 42.86 | 43.22 | 15.56 | 13.74 | 15.27 |
| LLaVA-vicuna-13b | Image (MV) | 44.29 | 41.85 | 16.67 | 16.26 | 17.58 |

TABLE IX: **NeRF brief captioning on the HST dataset**. All methods trained on ShapeNeRF-Text training set. Best results are in **bold**, runner-up is underlined. (FV: front-view, MV: multi-view)

| Model | Modality | S-BERT | SimCSE | BLEU-1 | ROUGE-L | METEOR |
|--------------------|-------------|--------------|--------------|--------------|--------------|--------------|
| GPT4Point-Opt-2.7b | Point cloud | 30.50 | 31.08 | 8.12 | 12.35 | 11.62 |
| PointLLM-7b | Point cloud | <u>44.65</u> | <u>44.68</u> | 8.91 | 12.33 | <u>12.64</u> |
| LLaNA-7b | NeRF | 65.42 | 66.44 | 19.63 | 23.39 | 23.46 |
| LLaVA-vicuna-13b | Image (FV) | 33.79 | 42.66 | 10.28 | 13.22 | 12.19 |
| LLaVA-vicuna-13b | Image (MV) | 34.45 | 42.54 | <u>11.04</u> | 12.36 | 11.48 |

the zero-shot classification performance of LLaVA-13b, which turns out to be the best model for this task, followed by LLaNA-13b. Similar to the brief captioning task, image-based models tend to outperform point cloud-based models on this classification task. This performance pattern aligns with the requirements of these tasks. For brief captioning and classification, which primarily require high-level understanding and concise outputs, image-based models excel by leveraging visual features directly from 2D views, where the nature of the object and its appearance are readily accessible. However, the pattern reverses for detailed captioning and Q&A tasks, where geometric precision and spatial understanding become crucial. These tasks often require reasoning about specific object parts, their relationships, and fine-grained spatial details - information that is inherently preserved in point cloud representations. While image-based models might struggle with occlusions and loss of information due to the chosen vantage points, point cloud-based approaches can directly reason about the complete 3D geometry, leading to more accurate and detailed responses.

B. Ablation study on training data

In this section, we run an ablation study where we train from scratch some methods on the same training set, i.e. ShapeNeRF-Text. This is done to assess the influence of the training set on the results. Due to the considerable computational resources required for training these models, we evaluated a subset of baselines using their official training code. Accordingly, we followed their protocol, which, for all methods, keeps the modality-specific encoder frozen and trains an adaptor. In PointLLM and LLaVA, the LLM is finetuned during an additional training stage.

Tables VIII, IX, X, XI and XII report results for both LLaNA and the baselines trained solely on ShapeNeRF-Text. We notice that these baselines exhibit different behaviors to their pre-trained counterparts, with LLaVA performing significantly worse and PointLLM showing clear improvements. As for GPT4Point, we observe greater variability across metrics; however, overall, it shows no significant benefit from training

TABLE X: **NeRF detailed captioning on ShapeNeRF-Text**. All methods trained on ShapeNeRF-Text training set. Best results are in **bold**, runner-up is underlined. (FV: front-view, MV: multi-view)

| Model | Modality | S-BERT | SimCSE | BLEU-1 | ROUGE-L | METEOR |
|--------------------|-------------|--------------|--------------|--------------|--------------|--------------|
| GPT4Point-Opt-2.7b | Point cloud | 41.33 | 40.52 | 14.48 | 19.15 | 13.80 |
| PointLLM-7b | Point cloud | <u>67.30</u> | <u>59.56</u> | <u>15.39</u> | 21.42 | 11.37 |
| LLaNA-7b | NeRF | 75.83 | 77.92 | 20.22 | 33.80 | 21.20 |
| LLaVA-vicuna-13b | Image (FV) | 44.69 | 42.31 | 10.08 | 23.46 | 12.70 |
| LLaVA-vicuna-13b | Image (MV) | 45.72 | 42.49 | 12.17 | <u>23.48</u> | <u>14.25</u> |

TABLE XI: **NeRF single-round Q&A on ShapeNeRF-Text**. All methods trained on ShapeNeRF-Text training set. Best results are in **bold**, runner-up is underlined. (FV: front-view, MV: multi-view)

| Model | Modality | S-BERT | SimCSE | BLEU-1 | ROUGE-L | METEOR |
|--------------------|-------------|--------------|--------------|--------------|--------------|--------------|
| GPT4Point-Opt-2.7b | Point cloud | 22.22 | 28.66 | 8.76 | 13.46 | 14.19 |
| PointLLM-7b | Point cloud | <u>79.24</u> | <u>80.38</u> | <u>46.00</u> | <u>52.60</u> | <u>42.36</u> |
| LLaNA-7b | NeRF | 81.94 | 82.43 | 47.73 | 54.97 | 51.78 |
| LLaVA-vicuna-13b | Image (FV) | 56.29 | 62.36 | 26.87 | 29.55 | 30.49 |
| LLaVA-vicuna-13b | Image (MV) | 56.42 | 64.47 | 25.41 | 30.09 | 32.04 |

TABLE XII: **Zero-shot NeRF classification on ShapeNeRF-Text**. All methods trained on ShapeNeRF-Text training set. Best results are in **bold**, runner-up is underlined. (FV: front-view, MV: multi-view)

| Model | Modality | Accuracy (%) |
|--------------------|-------------|--------------|
| GPT4Point-Opt-2.7b | Point cloud | 26.30 |
| PointLLM-7b | Point cloud | <u>49.69</u> |
| LLaNA-7b | NeRF | 69.06 |
| LLaVA-vicuna-13b | Image (FV) | 36.49 |
| LLaVA-vicuna-13b | Image (FV) | 39.27 |

on ShapeNeRF-Text. Also in this scenario, LLaNA yields the best performance compared to all baselines.

C. Is the LLM all you need?

Finally, we investigate how LLAMA 2, the LLM on which LLaNA relies, performs on NeRF-language tasks. For this evaluation protocol, the LLM, finetuned during the second training stage of LLaNA, is provided with questions belonging to our datasets, requiring it to generate correct answers without access to NeRF data. Consequently, its predictions rely solely on textual patterns present in the training set. These experiments offer valuable insights into the language annotations in ShapeNeRF-Text and ObjNeRF-Text, as well as the impact of different LLM sizes. Results are shown in Table XIII. Comparing this table with the ones reporting the results of LLaNA, we observe a significant performance gap between LLaNA and LLAMA. For instance, using the Sentence-BERT metric, LLaNA achieves scores of 75.09 and 75.51 on the brief and detailed captioning tasks of ShapeNeRF-Text, respectively, while LLAMA-13B attains only 29.29 and 40.20. This corresponds to performance drops of approximately 61% and 47%. Similarly, for the brief captioning task on ObjNeRF-Text, the performance drop is around 45% on the PointLLM test set and 47% on the GPT4Point test set. These substantial gaps indicate that ShapeNeRF-Text and ObjNeRF-Text provide language tasks that require access to 3D object information. Without

TABLE XIII: Language-only baselines NeRF captioning and NeRF single-round Q&A.

(Shape: ShapeNeRF-Text, Obja-P: ObjaNeRF-Text PointLLM test set, Obja-G: ObjaNeRF-Text GPT4Point test set)

| Model | Task | Dataset | SBERT | SimCSE | BLEU-1 | ROUGE-L | METEOR |
|-----------|----------|---------|-------|--------|--------|---------|--------|
| LLaMA-7b | brief | Shape | 31.08 | 27.44 | 22.13 | 19.39 | 17.44 |
| LLaMA-13b | brief | Shape | 29.29 | 24.69 | 16.95 | 18.93 | 13.85 |
| LLaMA-7b | brief | HST | 26.05 | 21.48 | 13.85 | 14.74 | 10.48 |
| LLaMA-13b | brief | HST | 26.83 | 21.44 | 13.19 | 15.30 | 10.12 |
| LLaMA-7b | brief | Obja-P | 28.20 | 29.33 | 10.37 | 13.59 | 12.95 |
| LLaMA-13b | brief | Obja-P | 23.19 | 21.29 | 10.25 | 13.45 | 10.91 |
| LLaMA-7b | brief | Obja-G | 23.82 | 21.70 | 13.21 | 16.79 | 13.50 |
| LLaMA-13b | brief | Obja-G | 23.43 | 19.54 | 14.18 | 17.40 | 13.81 |
| LLaMA-7b | detailed | Shape | 37.51 | 32.47 | 9.66 | 16.67 | 9.67 |
| LLaMA-13b | detailed | Shape | 40.20 | 35.80 | 11.35 | 18.82 | 11.29 |
| LLaMA-7b | Q&A | Shape | 76.89 | 76.61 | 42.01 | 49.74 | 45.69 |
| LLaMA-13b | Q&A | Shape | 76.85 | 76.79 | 42.30 | 49.92 | 45.86 |

the information from the NeRF token, the LLM is not able to provide correct descriptions. Therefore, our datasets can be used as reliable benchmarks for evaluating NeRF-language tasks. With regards to the single-round Q&A annotations, LLaMA-2 can answer correctly to a large set of questions leading to a limited performance gap with LLaNA: from 81.05 to 76.85, corresponding to a relative decrease of 5%. This relatively small difference can be attributed to the nature of the questions themselves: many of them rely on common sense and general object knowledge rather than specific 3D object information. For instance, questions like *How can the filing cabinet be used to organize office documents?*, *What is a suitable use for this table?* can be answered without detailed information from the corresponding 3D objects. These types of questions were deliberately included to preserve the strong reasoning capabilities of LLaMA while creating more natural and comprehensive conversations. An additional noteworthy finding concerns the relationship between LLM size and performance on NeRF-language tasks. As discussed previously, using a larger LLM does not significantly improve the performance of LLaNA. This pattern is also evident in Table XIII, where LLaMA-7b and LLaMA-13b provide very similar results on ShapeNeRF-Text and ObjaNeRF-Text. This suggests that the ability of the model to process and comprehend 3D object inputs - through its pre-trained encoder and projection layers - is more important than the size of the LLM.

VI. LIMITATIONS AND FUTURE DIRECTIONS

Despite the promising results of LLaNA, our work is the first study in this direction and some limitations are yet to be addressed. The first limitation is that `nf2vec` can only process MLPs, which restricts our model to MLP-only NeRFs. However, thanks to the rapid advancements in meta-networks, it may become very soon possible to extend LLaNA to more complex NeRF architectures, such as InstantNGP [38]. For instance, the approach by [16] suggests the feasibility of processing various input architectures, although it is currently limited to small networks. The second shortcoming is that our framework has been tested solely on object-centric NeRFs. Expanding its application to NeRFs representing entire scenes would be a compelling direction for future research.

VII. CONCLUDING REMARKS

This paper addressed the novel task of creating a language assistant for NeRF. We have tackled this problem by leveraging recent advances in MLLMs and meta-networks processing neural fields. We have shown that it is feasible and effective to directly process the weights of a NeRF to project it into the input embedding space of an LLM. Building on our previous work [17], we have presented ObjaNeRF-Text, a benchmark for NeRF-language understanding that includes 280K annotated NeRFs with text-based conversations. Furthermore, we have scaled LLaNA to a larger LLM and conducted a detailed analysis of the impact of model size on NeRF-language performance. Finally, we have extended such analysis to existing MLLMs, offering insights into the scalability and effectiveness of different architectures.

ACKNOWLEDGEMENTS

We acknowledge IS CRA for awarding this project access to the LEONARDO supercomputer, owned by the EuroHPC Joint Undertaking, hosted by CINECA (Italy).

This work was partially funded by “FSE+ 2021-2027 ai sensi dell’art. 24, comma 3, lett. a), della Legge 240/2010 e s.m.i. e del D.G.R. 693/2023 (RIF. PA: 2023-20090/RER - CUP: J19J23000730002)”.

REFERENCES

- [1] J. D. M.-W. C. Kenton and L. K. Toutanova, “Bert: Pre-training of deep bidirectional transformers for language understanding,” in *Proceedings of naacL-HLT*, vol. 1. Minneapolis, Minnesota, 2019, p. 2.
- [2] C. Raffel, N. Shazeer, A. Roberts, K. Lee, S. Narang, M. Matena, Y. Zhou, W. Li, and P. J. Liu, “Exploring the limits of transfer learning with a unified text-to-text transformer,” *Journal of machine learning research*, vol. 21, no. 140, pp. 1–67, 2020.
- [3] J. Achiam, S. Adler, S. Agarwal, L. Ahmad, I. Akkaya, F. L. Aleman, D. Almeida, J. Altenschmidt, S. Altman, S. Anadkat *et al.*, “Gpt-4 technical report,” *arXiv preprint arXiv:2303.08774*, 2023.
- [4] H. Touvron, T. Lavril, G. Izacard, X. Martinet, M.-A. Lachaux, T. Lacroix, B. Rozière, N. Goyal, E. Hambro, F. Azhar *et al.*, “Llama: Open and efficient foundation language models,” *arXiv preprint arXiv:2302.13971*, 2023.
- [5] D. Driess, F. Xia, M. S. Sajjadi, C. Lynch, A. Chowdhery, B. Ichter, A. Wahid, J. Tompson, Q. Vuong, T. Yu *et al.*, “Palm-e: An embodied multimodal language model,” in *International Conference on Machine Learning*. PMLR, 2023, pp. 8469–8488.
- [6] R. Zhang, J. Han, C. Liu, P. Gao, A. Zhou, X. Hu, S. Yan, P. Lu, H. Li, and Y. Qiao, “Llama-adapter: Efficient fine-tuning of language models with zero-init attention,” *arXiv preprint arXiv:2303.16199*, 2023.
- [7] H. Liu, C. Li, Q. Wu, and Y. J. Lee, “Visual instruction tuning,” *Advances in neural information processing systems*, vol. 36, 2024.
- [8] W. Dai, J. Li, D. Li, A. M. H. Tiong, J. Zhao, W. Wang, B. Li, P. N. Fung, and S. Hoi, “Instructblip: Towards general-purpose vision-language models with instruction tuning,” *Advances in Neural Information Processing Systems*, vol. 36, 2024.
- [9] G. Chen, Y.-D. Zheng, J. Wang, J. Xu, Y. Huang, J. Pan, Y. Wang, Y. Wang, Y. Qiao, T. Lu *et al.*, “Videollm: Modeling video sequence with large language models,” *arXiv preprint arXiv:2305.13292*, 2023.
- [10] R. Xu, X. Wang, T. Wang, Y. Chen, J. Pang, and D. Lin, “Pointllm: Empowering large language models to understand point clouds,” *arXiv preprint arXiv:2308.16911*, 2023.
- [11] Z. Qi, Y. Fang, Z. Sun, X. Wu, T. Wu, J. Wang, D. Lin, and H. Zhao, “Gpt4point: A unified framework for point-language understanding and generation,” in *CVPR*, 2024.
- [12] Y. Hong, H. Zhen, P. Chen, S. Zheng, Y. Du, Z. Chen, and C. Gan, “3d-LLM: Injecting the 3d world into large language models,” in *Thirty-seventh Conference on Neural Information Processing Systems*, 2023. [Online]. Available: <https://openreview.net/forum?id=YQA28p7qNz>

- [13] B. Mildenhall, P. P. Srinivasan, M. Tancik, J. T. Barron, R. Ramamoorthi, and R. Ng, "Nerf: Representing scenes as neural radiance fields for view synthesis," in *European conference on computer vision*. Springer, 2020, pp. 405–421.
- [14] B. Hu, J. Huang, Y. Liu, Y.-W. Tai, and C.-K. Tang, "Nerf-rpn: A general framework for object detection in nerfs," in *Proceedings of the IEEE/CVF Conference on Computer Vision and Pattern Recognition*, 2023, pp. 23 528–23 538.
- [15] P. Zama Ramirez, L. De Luigi, D. Sirocchi, A. Cardace, R. Spezialetti, F. Ballerini, S. Salti, and L. Di Stefano, "Deep learning on 3D neural fields," *arXiv preprint arXiv:2312.13277*, 2023.
- [16] D. Lim, H. Maron, M. T. Law, J. Lorraine, and J. Lucas, "Graph metanetworks for processing diverse neural architectures," in *The Twelfth International Conference on Learning Representations*, 2024. [Online]. Available: <https://openreview.net/forum?id=ijK5hyxx0n>
- [17] A. Amaduzzi, P. Z. Ramirez, G. Lisanti, S. Salti, and L. Di Stefano, "Llana: Large language and nerf assistant," *arXiv preprint arXiv:2406.11840*, 2024.
- [18] A. Amaduzzi, G. Lisanti, S. Salti, and L. Di Stefano, "Looking at words and points with attention: a benchmark for text-to-shape coherence," in *2023 IEEE/CVF International Conference on Computer Vision Workshops (ICCVW)*. IEEE Computer Society, 2023, pp. 2860–2869.
- [19] M. Deitke, D. Schwenk, J. Salvador, L. Weihs, O. Michel, E. VanderBilt, L. Schmidt, K. Ehsani, A. Kembhavi, and A. Farhadi, "Objaverse: A universe of annotated 3d objects," in *Proceedings of the IEEE/CVF Conference on Computer Vision and Pattern Recognition*, 2023, pp. 13 142–13 153.
- [20] P. Gao, J. Han, R. Zhang, Z. Lin, S. Geng, A. Zhou, W. Zhang, P. Lu, C. He, X. Yue *et al.*, "Llama-adapter v2: Parameter-efficient visual instruction model," *arXiv preprint arXiv:2304.15010*, 2023.
- [21] R. Girdhar, A. El-Nouby, Z. Liu, M. Singh, K. V. Alwala, A. Joulin, and I. Misra, "Imagebind: One embedding space to bind them all," in *Proceedings of the IEEE/CVF Conference on Computer Vision and Pattern Recognition*, 2023, pp. 15 180–15 190.
- [22] R. Huang, M. Li, D. Yang, J. Shi, X. Chang, Z. Ye, Y. Wu, Z. Hong, J. Huang, J. Liu *et al.*, "Audiotgt: Understanding and generating speech, music, sound, and talking head," in *Proceedings of the AAAI Conference on Artificial Intelligence*, vol. 38, no. 21, 2024, pp. 23 802–23 804.
- [23] M. Maaz, H. Rasheed, S. Khan, and F. S. Khan, "Video-chatgpt: Towards detailed video understanding via large vision and language models," *arXiv preprint arXiv:2306.05424*, 2023.
- [24] S. Huang, L. Dong, W. Wang, Y. Hao, S. Singhal, S. Ma, T. Lv, L. Cui, O. K. Mohammed, B. Patra *et al.*, "Language is not all you need: Aligning perception with language models," *Advances in Neural Information Processing Systems*, vol. 36, 2024.
- [25] Z. Peng, W. Wang, L. Dong, Y. Hao, S. Huang, S. Ma, and F. Wei, "Kosmos-2: Grounding multimodal large language models to the world," *arXiv preprint arXiv:2306.14824*, 2023.
- [26] B. Li, Y. Zhang, L. Chen, J. Wang, F. Pu, J. Yang, C. Li, and Z. Liu, "Mimic-it: Multi-modal in-context instruction tuning," *arXiv preprint arXiv:2306.05425*, 2023.
- [27] J. Bai, S. Bai, S. Yang, S. Wang, S. Tan, P. Wang, J. Lin, C. Zhou, and J. Zhou, "Qwen-vl: A frontier large vision-language model with versatile abilities," *arXiv preprint arXiv:2308.12966*, 2023.
- [28] J. Li, D. Li, S. Savarese, and S. Hoi, "Blip-2: Bootstrapping language-image pre-training with frozen image encoders and large language models," in *International conference on machine learning*. PMLR, 2023, pp. 19 730–19 742.
- [29] Z. Zhu, X. Ma, Y. Chen, Z. Deng, S. Huang, and Q. Li, "3d-vista: Pre-trained transformer for 3d vision and text alignment," *ICCV*, 2023.
- [30] Z. Guo, R. Zhang, X. Zhu, Y. Tang, X. Ma, J. Han, K. Chen, P. Gao, X. Li, H. Li *et al.*, "Point-bind & point-llm: Aligning point cloud with multi-modality for 3d understanding, generation, and instruction following," *arXiv preprint arXiv:2309.00615*, 2023.
- [31] Y. Hong, C. Lin, Y. Du, Z. Chen, J. B. Tenenbaum, and C. Gan, "3d concept learning and reasoning from multi-view images," in *Proceedings of the IEEE/CVF Conference on Computer Vision and Pattern Recognition (CVPR)*, June 2023, pp. 9202–9212.
- [32] R. Martin-Brualla, N. Radwan, M. S. Sajjadi, J. T. Barron, A. Dosovitskiy, and D. Duckworth, "Nerf in the wild: Neural radiance fields for unconstrained photo collections," in *Proceedings of the IEEE/CVF Conference on Computer Vision and Pattern Recognition*, 2021, pp. 7210–7219.
- [33] B. Poole, A. Jain, J. T. Barron, and B. Mildenhall, "Dreamfusion: Text-to-3d using 2d diffusion," in *The Eleventh International Conference on Learning Representations*, 2022.
- [34] L. Yen-Chen, P. Florence, J. T. Barron, T.-Y. Lin, A. Rodriguez, and P. Isola, "Nerf-supervision: Learning dense object descriptors from neural radiance fields," in *2022 international conference on robotics and automation (ICRA)*. IEEE, 2022, pp. 6496–6503.
- [35] A. Chen, Z. Xu, A. Geiger, J. Yu, and H. Su, "Tensorf: Tensorial radiance fields," in *European Conference on Computer Vision (ECCV)*, 2022.
- [36] C. Sun, M. Sun, and H.-T. Chen, "Direct voxel grid optimization: Super-fast convergence for radiance fields reconstruction," in *Proceedings of the IEEE/CVF Conference on Computer Vision and Pattern Recognition*, 2022, pp. 5459–5469.
- [37] S. Fridovich-Keil, A. Yu, M. Tancik, Q. Chen, B. Recht, and A. Kanazawa, "Plenoxels: Radiance fields without neural networks," *2022 IEEE/CVF Conference on Computer Vision and Pattern Recognition (CVPR)*, Jun 2022. [Online]. Available: <http://dx.doi.org/10.1109/CVPR52688.2022.00542>
- [38] T. Müller, A. Evans, C. Schied, and A. Keller, "Instant neural graphics primitives with a multiresolution hash encoding," *ACM Trans. Graph.*, vol. 41, no. 4, pp. 102:1–102:15, Jul. 2022. [Online]. Available: <https://doi.org/10.1145/3528223.3530127>
- [39] H. Seo, H. Kim, G. Kim, and S. Y. Chun, "Ditto-nerf: Diffusion-based iterative text to omni-directional 3d model," 2023.
- [40] G. Metzger, E. Richardson, O. Patashnik, R. Giryes, and D. Cohen-Or, "Latent-nerf for shape-guided generation of 3d shapes and textures," in *Proceedings of the IEEE/CVF Conference on Computer Vision and Pattern Recognition (CVPR)*, June 2023, pp. 12 663–12 673.
- [41] K. Jo, G. Shim, S. Jung, S. Yang, and J. Choo, "Cg-nerf: Conditional generative neural radiance fields for 3d-aware image synthesis," in *Proceedings of the IEEE/CVF Winter Conference on Applications of Computer Vision (WACV)*, January 2023, pp. 724–733.
- [42] B. Sen, G. Singh, A. Agarwal, R. Agaram, M. Krishna, and S. Sridhar, "Hyp-nerf: Learning improved nerf priors using a hypernetwork," in *Advances in Neural Information Processing Systems*, A. Oh, T. Naumann, A. Globerson, K. Saenko, M. Hardt, and S. Levine, Eds., vol. 36. Curran Associates, Inc., 2023, pp. 51 050–51 064. [Online]. Available: https://proceedings.neurips.cc/paper_files/paper/2023/file/a03037317560b8c5f2fb4b6466d4c439-Paper-Conference.pdf
- [43] J. Li, S. Liu, Z. Liu, Y. Wang, K. Zheng, J. Xu, J. Li, and J. Zhu, "Instructpix2neRF: Instructed 3d portrait editing from a single image," in *The Twelfth International Conference on Learning Representations*, 2024. [Online]. Available: <https://openreview.net/forum?id=XLxhINXtQk>
- [44] H.-H. Lee and A. X. Chang, "Understanding pure clip guidance for voxel grid nerf models," 2022.
- [45] C. Wang, M. Chai, M. He, D. Chen, and J. Liao, "Clip-nerf: Text-and-image driven manipulation of neural radiance fields," in *Proceedings of the IEEE/CVF Conference on Computer Vision and Pattern Recognition*, 2022, pp. 3835–3844.
- [46] S. Hwang, J. Hyung, D. Kim, M.-J. Kim, and J. Choo, "Faceclipnerf: Text-driven 3d face manipulation using deformable neural radiance fields," in *Proceedings of the IEEE/CVF International Conference on Computer Vision (ICCV)*, October 2023, pp. 3469–3479.
- [47] H. Song, S. Choi, H. Do, C. Lee, and T. Kim, "Blending-nerf: Text-driven localized editing in neural radiance fields," in *Proceedings of the IEEE/CVF International Conference on Computer Vision (ICCV)*, October 2023, pp. 14 383–14 393.
- [48] C. Wang, R. Jiang, M. Chai, M. He, D. Chen, and J. Liao, "Nerf-art: Text-driven neural radiance fields stylization," *IEEE Transactions on Visualization and Computer Graphics*, pp. 1–15, 2023.
- [49] C. Sun, Y. Liu, J. Han, and S. Gould, "Nerfeditor: Differentiable style decomposition for 3d scene editing," in *Proceedings of the IEEE/CVF Winter Conference on Applications of Computer Vision (WACV)*, January 2024, pp. 7306–7315.
- [50] A. Haque, M. Tancik, A. A. Efros, A. Holynski, and A. Kanazawa, "Instruct-nerf2nerf: Editing 3d scenes with instructions," in *Proceedings of the IEEE/CVF International Conference on Computer Vision (ICCV)*, October 2023, pp. 19 740–19 750.
- [51] Y. Yu, R. Wu, Y. Men, S. Lu, M. Cui, X. Xie, and C. Miao, "Morphnerf: Text-guided 3d-aware editing via morphing generative neural radiance fields," *IEEE Transactions on Multimedia*, pp. 1–13, 2024.
- [52] J. Zhuang, C. Wang, L. Lin, L. Liu, and G. Li, "Dreameditor: Text-driven 3d scene editing with neural fields," in *SIGGRAPH Asia 2023 Conference Papers*, 2023, pp. 1–10.
- [53] H. Bai, Y. Lyu, L. Jiang, S. Li, H. Lu, X. Lin, and L. Wang, "Componerf: Text-guided multi-object compositional nerf with editable 3d scene layout," *arXiv preprint arXiv:2303.13843*, 2023.
- [54] A. Mirzaei, T. Aumentado-Armstrong, M. A. Brubaker, J. Kelly, A. Levinstein, K. G. Derpanis, and I. Gilitschenski, "Reference-guided

- controllable inpainting of neural radiance fields,” in *Proceedings of the IEEE/CVF International Conference on Computer Vision (ICCV)*, October 2023, pp. 17 815–17 825.
- [55] J. Kerr, C. M. Kim, K. Goldberg, A. Kanazawa, and M. Tancik, “Lerf: Language embedded radiance fields,” in *International Conference on Computer Vision (ICCV)*, 2023.
- [56] S. Kobayashi, E. Matsumoto, and V. Sitzmann, “Decomposing nerf for editing via feature field distillation,” in *Advances in Neural Information Processing Systems*, S. Koyejo, S. Mohamed, A. Agarwal, D. Belgrave, K. Cho, and A. Oh, Eds., vol. 35. Curran Associates, Inc., 2022, pp. 23 311–23 330. [Online]. Available: https://proceedings.neurips.cc/paper_files/paper/2022/file/93f250215e4889119807b6fac3a57aec-Paper-Conference.pdf
- [57] F. Ballerini, P. Zama Ramirez, R. Mirabella, S. Salti, and L. Di Stefano, “Connecting nerfs, images, and text,” in *Proceedings of the IEEE/CVF Conference on Computer Vision and Pattern Recognition (CVPR) Workshops*, June 2024.
- [58] A. Radford, J. W. Kim, C. Hallacy, A. Ramesh, G. Goh, S. Agarwal, G. Sastry, A. Askell, P. Mishkin, J. Clark *et al.*, “Learning transferable visual models from natural language supervision,” in *International Conference on Machine Learning*. PMLR, 2021, pp. 8748–8763.
- [59] T. Unterthiner, D. Keysers, S. Gelly, O. Bousquet, and I. O. Tolstikhin, “Predicting neural network accuracy from weights,” *arXiv*, vol. abs/2002.11448, 2020.
- [60] K. Schürholt, D. Kostadinov, and D. Borth, “Self-supervised representation learning on neural network weights for model characteristic prediction,” in *Advances in Neural Information Processing Systems*, A. Beygelzimer, Y. Dauphin, P. Liang, and J. W. Vaughan, Eds., 2021. [Online]. Available: <https://openreview.net/forum?id=FID8buayXQT>
- [61] B. Knyazev, M. Drozdal, G. W. Taylor, and A. Romero, “Parameter prediction for unseen deep architectures,” in *Advances in Neural Information Processing Systems*, A. Beygelzimer, Y. Dauphin, P. Liang, and J. W. Vaughan, Eds., 2021. [Online]. Available: <https://openreview.net/forum?id=vqHak8NLk25>
- [62] F. Jaeckle and M. P. Kumar, “Generating adversarial examples with graph neural networks,” in *Uncertainty in Artificial Intelligence*. PMLR, 2021, pp. 1556–1564.
- [63] J. Lu and M. P. Kumar, “Neural network branching for neural network verification,” in *International Conference on Learning Representations*, 2020. [Online]. Available: <https://openreview.net/forum?id=B1evfa4tPB>
- [64] E. Dupont, H. Kim, S. A. Eslami, D. J. Rezende, and D. Rosenbaum, “From data to functa: Your data point is a function and you can treat it like one,” in *International Conference on Machine Learning*. PMLR, 2022, pp. 5694–5725.
- [65] L. De Luigi, A. Cardace, R. Spezialetti, P. Zama Ramirez, S. Salti, and L. Di Stefano, “Deep learning on implicit neural representations of shapes,” in *International Conference on Learning Representations (ICLR)*, 2023.
- [66] A. Cardace, P. Z. Ramirez, F. Ballerini, A. Zhou, S. Salti, and L. di Stefano, “Neural processing of tri-plane hybrid neural fields,” in *The Twelfth International Conference on Learning Representations*, 2024. [Online]. Available: <https://openreview.net/forum?id=zRkM6UcA22>
- [67] A. Navon, A. Shamsian, I. Achituv, E. Fetaya, G. Chechik, and H. Maron, “Equivariant architectures for learning in deep weight spaces,” in *International Conference on Machine Learning*, 2023.
- [68] A. Zhou, K. Yang, Y. Jiang, K. Burns, W. Xu, S. Sokota, J. Z. Kolter, and C. Finn, “Neural functional transformers,” *Advances in neural information processing systems*, vol. 37, 2023.
- [69] A. Zhou, K. Yang, K. Burns, A. Cardace, Y. Jiang, S. Sokota, J. Z. Kolter, and C. Finn, “Permutation equivariant neural functionals,” *Advances in neural information processing systems*, vol. 37, 2023.
- [70] A. Zhou, C. Finn, and J. Harrison, “Universal neural functionals,” *arXiv preprint arXiv:2402.05232*, 2024.
- [71] R. Hecht-Nielsen, “On the algebraic structure of feedforward network weight spaces,” in *Advanced Neural Computers*. Elsevier, 1990, pp. 129–135.
- [72] M. Kofinas, B. Knyazev, Y. Zhang, Y. Chen, G. J. Burghouts, E. Gavves, C. G. Snoek, and D. W. Zhang, “Graph neural networks for learning equivariant representations of neural networks,” in *The Twelfth International Conference on Learning Representations*, 2024.
- [73] R. Girshick, “Fast r-cnn,” in *Proceedings of the IEEE international conference on computer vision*, 2015, pp. 1440–1448.
- [74] S. Ioffe and C. Szegedy, “Batch normalization: Accelerating deep network training by reducing internal covariate shift,” in *International conference on machine learning*. pmlr, 2015, pp. 448–456.
- [75] A. Vaswani, N. Shazeer, N. Parmar, J. Uszkoreit, L. Jones, A. N. Gomez, Ł. Kaiser, and I. Polosukhin, “Attention is all you need,” in *Advances in Neural Information Processing Systems*, I. Guyon, U. V. Luxburg, S. Bengio, H. Wallach, R. Fergus, S. Vishwanathan, and R. Garnett, Eds., vol. 30. Curran Associates, Inc., 2017. [Online]. Available: https://proceedings.neurips.cc/paper_files/paper/2017/file/3f5ee243547dee91fbd053c1c4a845aa-Paper.pdf
- [76] A. X. Chang, T. Funkhouser, L. Guibas, P. Hanrahan, Q. Huang, Z. Li, S. Savarese, M. Savva, S. Song, H. Su *et al.*, “Shapenet: An information-rich 3d model repository,” *arXiv preprint arXiv:1512.03012*, 2015.
- [77] Q. Zuo, X. Gu, Y. Dong, Z. Zhao, W. Yuan, L. Qiu, L. Bo, and Z. Dong, “High-fidelity 3d textured shapes generation by sparse encoding and adversarial decoding,” in *European Conference on Computer Vision*, 2024.
- [78] T. Luo, C. Rockwell, H. Lee, and J. Johnson, “Scalable 3d captioning with pretrained models,” *Advances in Neural Information Processing Systems*, vol. 36, 2024.
- [79] N. Reimers and I. Gurevych, “Sentence-bert: Sentence embeddings using siamese bert-networks,” *arXiv preprint arXiv:1908.10084*, 2019.
- [80] T. Gao, X. Yao, and D. Chen, “Simcse: Simple contrastive learning of sentence embeddings,” in *2021 Conference on Empirical Methods in Natural Language Processing, EMNLP 2021*. Association for Computational Linguistics (ACL), 2021, pp. 6894–6910.
- [81] K. Papineni, S. Roukos, T. Ward, and W.-J. Zhu, “Bleu: a method for automatic evaluation of machine translation,” in *Proceedings of the 40th annual meeting of the Association for Computational Linguistics*, 2002, pp. 311–318.
- [82] C.-Y. Lin, “Rouge: A package for automatic evaluation of summaries,” in *Text summarization branches out*, 2004, pp. 74–81.
- [83] S. Banerjee and A. Lavie, “Meteor: An automatic metric for mt evaluation with improved correlation with human judgments,” in *Proceedings of the acl workshop on intrinsic and extrinsic evaluation measures for machine translation and/or summarization*, 2005, pp. 65–72.
- [84] J. Li, D. Li, S. Savarese, and S. Hoi, “BLIP-2: Bootstrapping language-image pre-training with frozen image encoders and large language models,” *arXiv preprint arXiv:2301.12597*, 2023.



Andrea Amaduzzi is a fourth-year PhD student at the Computer Vision Laboratory (CVLAB), University of Bologna. Prior to his doctoral studies, he worked as a Computer Vision Software Engineer at Datalogic. He authored several research papers covering a range of subjects, including 3D computer vision and multimodal learning.



Pierluigi Zama Ramirez received his PhD in Computer Science and Engineering in 2021. He has been a Research Intern at Google for 6 months and is currently a Post-Doc at the University of Bologna. He co-authored more than 20 publications on computer vision research topics such as semantic segmentation, depth estimation, optical flow, domain adaptation, virtual reality, and 3D computer vision.



Giuseppe Lisanti is currently an Associate Professor in the Department of Computer Science and Engineering at the University of Bologna. He has co-authored over 50 publications, with his primary research interests focus on computer vision and the application of deep learning to computer vision problems. He actively collaborates with other research centres and has participated in various roles in multiple research projects. In 2017, he received the Best Paper Award from the IEEE Computer Society Workshop on Biometrics.



Samuele Salti is currently an associate professor at the Department of Computer Science and Engineering (DISI) of the University of Bologna, Italy. His main research interest is computer vision, mainly 3D computer vision and machine/deep learning applied to computer vision problems. Dr. Salti has co-authored more than 60 publications and 8 international patents. In 2020, he co-founded the start-up eyecan.ai.



Luigi Di Stefano received a PhD degree in electronic engineering and computer science from the University of Bologna in 1994. He is a full professor at the Department of Computer Science and Engineering, University of Bologna, where he founded and led the Computer Vision Laboratory (CVLab). His research interests include image processing, computer vision, and machine/deep learning. He is the author of more than 150 papers and several patents. He has been a scientific consultant for major computer vision and machine learning companies.

He is a member of the IEEE Computer Society and the IAPR-IC.